

# A Radiative Neutrino Model

## Linking to

# A Monochromatic Gamma-ray Line

Seungwon Baek,<sup>1,\*</sup> Hiroshi Okada,<sup>2,†</sup> and Yuta Orikasa<sup>3,‡</sup>

<sup>1</sup>*School of Physics, KIAS, Seoul 130-722, Korea*

<sup>2</sup>*Physics Division, National Center for Theoretical Sciences, Hsinchu, Taiwan 300*

<sup>3</sup>*Institute of Experimental and Applied Physics,  
Czech Technical University, Prague 12800, Czech Republic*

(Dated: December 3, 2024)

## Abstract

We explore the possibility to explain the monochromatic Fermi-LAT anomaly at 42.7 GeV dark matter mass in the framework of radiatively induced neutrino mass model at two level. Here we prepare the Zee-Babu type scenario with  $Z_3$  discrete symmetry, in which we consider the neutrino oscillation data, lepton flavor violations, muon  $g - 2$ , and bosonic dark matter candidate. A  $\mu - e$  conversion rate, which can be tested in the near future experiment such as PRISM/PRIME, is estimated and its allowed range is shown through the global analysis.

Keywords:

---

\*Electronic address: swbaek@kias.re.kr

†Electronic address: macokada3hiroshi@cts.nthu.edu.tw

‡Electronic address: Yuta.Orikasa@utef.cvut.cz

	Lepton Fields			Scalar Fields			
	$L_L$	$e_R$	$N_{L/R}$	$\Phi$	$\eta$	$\chi$	$\chi^+$
$SU(2)_L$	<b>2</b>	<b>1</b>	<b>1</b>	<b>2</b>	<b>2</b>	<b>1</b>	<b>1</b>
$U(1)_Y$	$-\frac{1}{2}$	$-1$	$0$	$\frac{1}{2}$	$\frac{1}{2}$	$0$	$1$
$Z_3$	$1$	$1$	$\omega$	$1$	$\omega$	$\omega$	$\omega$

TABLE I: Contents of fermion and scalar fields and their charge assignments under  $SU(2)_L \times U(1)_Y \times Z_3$ .

## I. INTRODUCTION

Radiatively induced neutrino masses could be one of the promising scenarios to make a strong correlation between neutrinos and any fields that are introduced inside the loop. If one wants to introduce a dark matter (DM) candidate in one's model, its testability is enhanced due to the fact that the parameter space is strongly constrained by neutrino data. Especially two-loop induced models that we will focus on in this paper are widely studied in various aspects [1–34].

A smoking-gun signal for dark matter is monochromatic gamma ray. In this letter, we explain a possible anomaly of monochromatic photon at 42.7 GeV which can be explained by annihilating DM with cross section,  $5 \times 10^{-28} \text{ cm}^3/s (\text{BF}/1000)^{-1}$ , BF being boost factor [36], in the framework of Zee-Babu type of neutrino model. We estimate the lepton flavor violating (LFV)  $\mu - e$  conversion rate in *Titanium* nuclei that will be tested in the near future experiment such as PRISM/PRIME [37] as well as muon anomalous magnetic moment.

This paper is organized as follows. In Sec. II, we show our model, including neutrino sector, LFVs, muon anomalous magnetic moment. In Sec. III, we analyze bosonic DM candidate to explain relic density and direct detection. In Sec. IV, we present the results of numerical analysis. We conclude and discuss in Sec. V.

## II. MODEL SETUP

In this section, we introduce our model. We introduce a global  $Z_3$  symmetry in addition to the SM gauge symmetry. The particle contents and their charges under  $SU(2)_L \times U(1)_Y \times Z_3$

are shown in Tab. I. We add three family of iso-spin singlet vector-like neutral fermions  $N^1$ , an iso-spin doublet scalar  $\eta$ , and an isospin singlet scalar  $\chi$  to the SM fields. Due to  $Z_3$  symmetry, only the SM-like Higgs  $\Phi$ , has vacuum expectation value (VEV),  $\langle \Phi^0 \rangle = v/\sqrt{2}$  [21]. All the new particles,  $N$ ,  $\eta$ ,  $\chi$  and  $\chi^\pm$  are charged under  $Z_3$  with the same charge,  $\omega$ .

Then the relevant Lagrangian and Higgs potential under these symmetries are given by

$$\begin{aligned}
-\mathcal{L}_Y &= (y_\ell)_{ij} \bar{L}_{L_i} \Phi e_{R_j} + (y_\eta)_{ij} \bar{L}_{L_i} (i\sigma_2) \eta^* N_{R_j} + y_{N_{R_{ij}}} \bar{N}_{R_i}^c N_{R_j} \chi + y_{N_{L_{ij}}} \bar{N}_{L_i}^c N_{L_j} \chi \\
&\quad + (y_\chi)_{ij} \bar{N}_{L_i} e_{R_j} \chi^+ + M_{N_{ij}} \bar{N}_{L_i} N_{R_j} + \text{h.c.}, \\
\mathcal{V} &= m_\Phi^2 \Phi^\dagger \Phi + m_\eta^2 |\eta|^2 + m_\chi^2 |\chi|^2 + m_{\chi^\pm}^2 |\chi^\pm|^2 \\
&\quad + \mu(\eta^T (i\sigma_2) \Phi \chi^- + \text{h.c.}) + \mu_{\eta\chi} (\Phi^\dagger \eta \chi^* + \text{h.c.}) + \mu_\chi (\chi^3 + \text{h.c.}) \\
&\quad + \lambda_\Phi (\Phi^\dagger \Phi)^2 + \lambda_0 (\Phi^\dagger \eta \chi^2 + \text{h.c.}) + \lambda_\eta (\eta^\dagger \eta)^2 + \lambda_\chi (\chi^* \chi)^2 + \lambda_{\chi^\pm} (\chi^+ \chi^-)^2 + \lambda_{\Phi\eta} (\Phi^\dagger \Phi) (\eta^\dagger \eta) \\
&\quad + \lambda'_{\Phi\eta} |\Phi^\dagger \eta|^2 + \lambda_{\Phi\chi} (\Phi^\dagger \Phi) \chi^* \chi + \lambda_{\eta\chi} (\eta^\dagger \eta) \chi^* \chi \\
&\quad + \lambda_{\Phi\chi^\pm} (\Phi^\dagger \Phi) \chi^+ \chi^- + \lambda_{\eta\chi^\pm} (\eta^\dagger \eta) \chi^+ \chi^- + \lambda_{\chi\chi^\pm} (\chi^* \chi) \chi^+ \chi^-, \tag{II.1}
\end{aligned}$$

where  $\sigma_2$  is the second Pauli matrix,  $i, j = 1 - 3$ , and the first term of  $\mathcal{L}_Y$  can generate the SM charged-lepton masses  $m_\ell \equiv y_\ell v/\sqrt{2}$  after  $\Phi$  obtains VEV. We assume the  $N_i$ 's are the mass eigenstates, *i.e.*,  $M_{N_{ij}} = M_{N_i} \delta_{ij}$ . We work in the basis where all the coefficients are real and positive for simplicity. The scalar fields can be parameterized in the unitary gauge as follows:

$$\Phi = \begin{bmatrix} 0 \\ \frac{v+\phi}{\sqrt{2}} \end{bmatrix}, \quad \eta = \begin{bmatrix} \eta^+ \\ \eta \end{bmatrix}, \quad \chi, \quad \chi^\pm, \tag{II.2}$$

where  $\eta$  and  $\chi$  are complex inert neutral bosons,  $\chi^\pm$  is the singly charged boson,  $v \simeq 246$  GeV is VEV of the Higgs doublet, and  $\phi$  is the SM Higgs boson and with mass  $m_\phi \approx 125.5$  GeV.

Notice here that we have mixing between inert bosons through  $\mu_{\eta\chi}$  and  $\mu$ , the resulting

---

<sup>1</sup> The  $N_R$ 's are introduced to give masses to  $N$ 's.

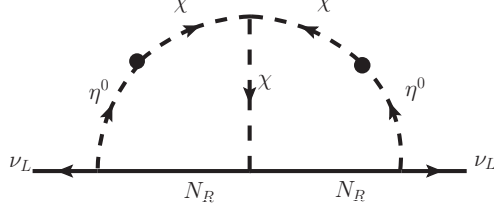


FIG. 1: The two-loop diagram the generation of neutrino masses. The blobs indicate the scalar mixing between  $\eta^0$  and  $\chi$ .

mass eigenvalues  $M_H$ , and rotation matrix being respectively given as

$$O_H^T M_H O_H = \begin{bmatrix} m_{H_1} & 0 \\ 0 & m_{H_2} \end{bmatrix}, \quad \begin{bmatrix} \chi \\ \eta \end{bmatrix} = O \begin{bmatrix} H_1 \\ H_2 \end{bmatrix} = \begin{bmatrix} \cos \alpha & \sin \alpha \\ -\sin \alpha & \cos \alpha \end{bmatrix} \begin{bmatrix} H_1 \\ H_2 \end{bmatrix}, \quad (\text{II.3})$$

$$V_C^T M_{H^\pm} V_C = \begin{bmatrix} m_{H_1^\pm} & 0 \\ 0 & m_{H_2^\pm} \end{bmatrix}, \quad \begin{bmatrix} \chi^\pm \\ \eta^\pm \end{bmatrix} = V_C \begin{bmatrix} H_1^\pm \\ H_2^\pm \end{bmatrix} = \begin{bmatrix} \cos \beta & \sin \beta \\ -\sin \beta & \cos \beta \end{bmatrix} \begin{bmatrix} H_1^\pm \\ H_2^\pm \end{bmatrix}, \quad (\text{II.4})$$

where  $(H_{1(2)}, H_{1(2)}^\pm)$  and  $(\alpha, \beta)$  are written in terms of Higgs potential, and we use the short hand notation  $s_{\alpha(\beta)}(c_{\alpha(\beta)})$  for  $\sin \alpha(\beta)(\cos \alpha(\beta))$  below <sup>2</sup>.

### A. Neutrino masses

The active neutrino mass matrix  $m_\nu$  is generated at two-loop level as shown in Figure 1, and its formula is given by

$$(m_\nu)_{ij} = \frac{12\sqrt{2}\mu_\chi s_\alpha^2 c_\alpha^2 (y_\eta)_{ia} (y_N)_{ab} (y_\eta)_{bj}^T}{(4\pi)^4} F_{II} \equiv (y_\eta)_{ia} (y'_N)_{ab} (y_\eta)_{bj}^T, \quad (\text{II.5})$$

$$F_{II} = \int \frac{[dx]}{z-1} \int [da] \left[ c_\alpha^2 \left[ \ln \left( \frac{\Delta_{111}}{\Delta_{112}} \right) - \ln \left( \frac{\Delta_{211}}{\Delta_{212}} \right) \right] + s_\alpha^2 \left[ \ln \left( \frac{\Delta_{222}}{\Delta_{221}} \right) - \ln \left( \frac{\Delta_{122}}{\Delta_{121}} \right) \right] \right], \quad (\text{II.6})$$

$$\Delta_{\ell mn} = -a \frac{xM_{N_b}^2 + ym_{H_n}^2 + zm_{H_m}^2}{z^2 - z} + bM_{N_a}^2 + cm_{H_\ell}^2, \quad (\text{II.7})$$

where  $[dx] \equiv dx dy dz \delta(x+y+z-1)$ ,  $[da] \equiv dadbdc\delta(a+b+c-1)$ , and we assume  $y_N \equiv y_{N_R} \approx y_{N_L}$ .

<sup>2</sup> See ref. [21] for details.

The active neutrino mass matrix,  $(m_\nu)_{ij}$ , can be generally diagonalized by the Pontecorvo-Maki-Nakagawa-Sakata (PMNS) mixing matrix  $V_{\text{MNS}}$  [38] as

$$(m_\nu)_{ij} = (V_{\text{MNS}}^* D_\nu V_{\text{MNS}}^\dagger)_{ij}, \quad D_\nu \equiv (0, m_{\nu_2}, m_{\nu_3}), \quad (\text{II.8})$$

$$V_{\text{MNS}} = \begin{bmatrix} c_{13}c_{12} & c_{13}s_{12} & s_{13}e^{-i\delta} \\ -c_{23}s_{12} - s_{23}s_{13}c_{12}e^{i\delta} & c_{23}c_{12} - s_{23}s_{13}s_{12}e^{i\delta} & s_{23}c_{13} \\ s_{23}s_{12} - c_{23}s_{13}c_{12}e^{i\delta} & -s_{23}c_{12} - c_{23}s_{13}s_{12}e^{i\delta} & c_{23}c_{13} \end{bmatrix}, \quad (\text{II.9})$$

where we assume one of three neutrino masses is zero with normal ordering, neglect the Majorana phase, and fix the Dirac phase  $\delta = -\pi/2$  in the numerical analysis for simplicity.

Then we apply the generalized Casas-Ibarra parametrization <sup>3</sup> to our analysis, where we use the observed neutrino oscillation with global fit [41]. Then Yukawa coupling  $y_\eta$  can be rewritten in terms of the following parameters:

$$y_\eta \approx V_{\text{MNS}}^* \sqrt{D_\nu} \mathcal{O}(\theta_{1,2,3}) (y_N'^{Ch})^{-1}, \quad (\text{II.10})$$

where  $\mathcal{O}(\theta_{1,2,3})$  is an arbitrary  $3 \times 3$  orthogonal matrix with three complex values  $\theta_{1,2,3}$ ,

and  $y_N'^{Ch}$  is Cholesky decomposed matrix. This matrix is a lower triangular matrix and satisfies the following relation (see appendix A),

$$y_N' = y_N'^{Ch} (y_N'^{Ch})^T. \quad (\text{II.11})$$

*Lepton flavor violations(LFVs)* arises from the terms  $y_\eta y_\chi$  at one-loop level <sup>4</sup>, and its

---

<sup>3</sup> In our case, the central matrix is not diagonal but the symmetric matrix which is proportional to  $y_N$ .

<sup>4</sup> Recently sophisticated analysis has been done by ref. [39, 40]

form is given by

$$\text{BR}(\ell_i \rightarrow \ell_j \gamma) = \frac{48\pi^3 C_{ij} \alpha_{\text{em}}}{G_{\text{F}}^2} \left( |(a_R^{\eta\chi})_{ij} + a_{R_{ij}}^\eta + a_{R_{ij}}^\chi|^2 + |(a_L^{\eta\chi})_{ij} + \epsilon_{ij}[a_{L_{ij}}^\eta + a_{L_{ij}}^\chi]|^2 \right), \quad (\text{II.12})$$

$$(a_R^{\eta\chi})_{ij} = (a_L^{\eta\chi})_{ij}^\dagger = -\frac{s_\beta c_\beta}{(4\pi)^2} \sum_{k=1,2,3} \frac{M_{N_k}}{m_{\ell_i}} (y_\eta)_{jk} (y_\chi)_{ki} \left( F_1(M_{N_k}, m_{H_1^\pm}) - F_1(M_{N_k}, m_{H_2^\pm}) \right), \quad (\text{II.13})$$

$$a_{R_{ij}}^\eta = a_{L_{ij}}^\eta = \sum_{k=1,2,3} \frac{(y_\eta)_{jk} (y_\eta^\dagger)_{ki}}{(4\pi)^2} \left[ s_\beta^2 F_{lfv}(M_{N_k}, m_{H_1^\pm}) + c_\beta^2 F_{lfv}(M_{N_k}, m_{H_2^\pm}) \right], \quad (\text{II.14})$$

$$a_{R_{ij}}^\chi = a_{L_{ij}}^\chi = \sum_{k=1,2,3} \frac{(y_\chi^\dagger)_{jk} (y_\chi)_{ki}}{(4\pi)^2} \left[ c_\beta^2 F_{lfv}(M_{N_k}, m_{H_1^\pm}) + s_\beta^2 F_{lfv}(M_{N_k}, m_{H_2^\pm}) \right], \quad (\text{II.15})$$

$$F_1(m_1, m_2) = \frac{m_1^2 + m_2^2}{2(m_1^2 - m_2^2)^2} - \frac{m_1^2 m_2^2}{(m_1^2 - m_2^2)^3} \log \frac{m_1^2}{m_2^2}, \quad (\text{II.16})$$

$$F_{lfv}(m_a, m_b) = \frac{2m_a^6 + 3m_a^4 m_b^2 - 6m_a^2 m_b^4 + 6m_b^6 + 12m_a^4 m_b^2 \ln(m_b/m_a)}{12(m_a^2 - m_b^2)^4}, \quad (\text{II.17})$$

where  $\epsilon_{ij} \equiv (m_{\ell_j}/m_{\ell_i})(\ll 1)$ ,  $\eta^\pm$  is the singly charged component of  $\eta$ ,  $G_{\text{F}} \approx 1.17 \times 10^{-5} [\text{GeV}]^{-2}$  is the Fermi constant,  $\alpha_{\text{em}} \approx 1/137$  is the fine structure constant,  $C_{21} \approx 1$ ,  $C_{31} \approx 0.1784$ , and  $C_{32} \approx 0.1736$ . Experimental upper bounds are respectively given by  $\text{BR}(\mu \rightarrow e\gamma) \lesssim 4.2 \times 10^{-13}$ ,  $\text{BR}(\tau \rightarrow e\gamma) \lesssim 3.3 \times 10^{-8}$ , and  $\text{BR}(\tau \rightarrow \mu\gamma) \lesssim 4.4 \times 10^{-8}$ .

The  $\mu - e$  conversion is obtained by using  $a_{R/L}$ , and its capture rate  $R$  is approximately given by <sup>5</sup>

$$R \approx \frac{C_{\mu e} |Z|^2}{\Gamma_{\text{cap}}} \left( |(a_R^{\eta\chi})_{ij} + a_{R_{ij}}^\eta + a_{R_{ij}}^\chi|^2 + |(a_L^{\eta\chi})_{ij} + \epsilon_{ij}[a_{L_{ij}}^\eta + a_{L_{ij}}^\chi]|^2 \right), \quad C_{\mu e} \approx 4\alpha_{\text{em}}^5 \frac{Z_{\text{eff}}^4 |F(q)|^2 m_\mu^5}{Z}, \quad (\text{II.18})$$

where  $Z$ ,  $Z_{\text{eff}}$ ,  $F(q)$ , and  $R$  are given in table II.

Here let us define  $Y \equiv \frac{R}{\text{BR}(\mu \rightarrow e\gamma)}$ , since their flavor structures are same. Then it is given by

$$Y \approx 1.22 \times 10^{-24} \left( \frac{Z Z_{\text{eff}}^4 |F(q)|^2}{\Gamma_{\text{cap}}} \right). \quad (\text{II.19})$$

Depending on the nuclei,  $Y \approx \mathcal{O}(0.1)$ , as is listed in table II. It suggests that each constraint of the  $\mu - e$  conversion is always satisfied once we satisfy the constraint of  $\mu \rightarrow e\gamma$ . We will discuss the sensitivity of future experiments,  $R_{Ti}$  and  $R_{Al}$ , in the numerical analysis.

<sup>5</sup> We neglect the contribution to the Z-penguin diagram due to suppression factor  $(m_\ell/M_N)^2$ .

Nucleus $\frac{A}{Z}N$	$Z_{\text{eff}}$	$ F(-m_\mu^2) $	$ \Gamma_{\text{capt}}(10^6 \text{sec}^{-1}) $	Experimental bound (Future bound)	$Y \equiv \frac{R}{\text{BR}(\mu \rightarrow e\gamma)}$
${}_{13}^{27}\text{Al}$	11.5	0.64	0.7054	$(R_{\text{Al}} \lesssim 10^{-16})$ [42]	0.25
${}_{22}^{48}\text{Ti}$	17.6	0.54	2.59	$R_{\text{Ti}} \lesssim 4.3 \times 10^{-12}$ [43] ( $\lesssim 10^{-18}$ [37])	0.44
${}_{79}^{197}\text{Au}$	33.5	0.16	13.07	$R_{\text{Au}} \lesssim 7 \times 10^{-13}$ [44]	0.36
${}_{82}^{208}\text{Pb}$	34	0.15	13.45	$R_{\text{Pb}} \lesssim 4.6 \times 10^{-11}$ [45]	0.34

TABLE II: Summary for the the  $\mu$ - $e$  conversion in various nuclei:  $Z$ ,  $Z_{\text{eff}}$ ,  $F(q)$ ,  $\Gamma_{\text{capt}}$ , and the bounds on the capture rate  $R$ .

*New contributions to the muon anomalous magnetic moment (muon  $g - 2$ )* is given by

$$\Delta a_\mu \approx -m_\mu [(a_R^{\eta\chi})_{\mu\mu} + a_{R\mu\mu}^\eta + a_{R\mu\mu}^\chi + (a_L^{\eta\chi})_{\mu\mu} + a_{L\mu\mu}^\eta + a_{L\mu\mu}^\chi], \quad (\text{II.20})$$

where only the terms  $(a_{R(L)}^{\eta\chi})_{\mu\mu}$  are positive contributions to the muon  $g - 2$ . Thus we expect that  $a_{R(L)\mu\mu}^\eta, a_{R(L)\mu\mu}^\chi \ll (a_{R(L)}^{\eta\chi})_{\mu\mu}$  in the numerical analysis. The experimental value is the order of  $\mathcal{O}(10^{-9})$  [35].

### III. DARK MATTER

Here we consider  $H_1(\equiv X)$  as the dark matter(DM) candidate, which is a complex scalar. Since we consider the anomaly in the photon line-like signature at  $M_X \approx 43$  GeV reported by Fermi-LAT experiment [36], allowed DM annihilation modes are kinematically restricted to  $XX^{(*)} \rightarrow b\bar{b}, \ell\bar{\ell}, \nu\bar{\nu}$ .

*Relic density of DM:* Here we discuss the relic density of DM. Annihilation channels to explain the relic density are  $XX^{(*)} \rightarrow b\bar{b}, \ell\bar{\ell}, \nu\bar{\nu}$ , and their cross sections are respectively

given by

$$\sigma v_{\text{rel}} \approx \sum_{f=X^{(*)},b,\nu} \int_0^\pi \sin \theta d\theta \frac{|M(XX^* \rightarrow f\bar{f})|^2}{16\pi s} \sqrt{1 - \frac{4m_f^2}{s}}, \quad (\text{III.1})$$

$$\begin{aligned} |M(XX^* \rightarrow \nu_i \bar{\nu}_j)|^2 &\approx s_\alpha^4 \left| \frac{(y_\eta)_{ia} (y_\eta^\dagger)_{aj}}{t - M_{N_a}^2} \right|^2 M_X^4 \sin^2 \theta v_{\text{rel}}^2 + 4C_Z^2 M_X^4 (A_{L\nu}^2 + A_{R\nu}^2) \sin^2 \theta v_{\text{rel}}^2 \\ &+ 4 \frac{M_X^4 s_\theta^2 s_\alpha^2 A_{L\nu} (y_\eta)_{ia} (y_\eta^\dagger)_{aj} C_Z}{t - M_{N_a}^2} v_{\text{rel}}^2, \end{aligned} \quad (\text{III.2})$$

$$|M(XX^* \rightarrow f\bar{f})|^2 \approx 2C_f M_X^2 [4C_\phi^2 + (C_\phi^2 + 2(A_{L_f}^2 + A_{R_f}^2)C_Z^2 \sin^2 \theta M_X^2) v_{\text{rel}}^2], \quad (\text{III.3})$$

$$\begin{aligned} C_\phi &\equiv \frac{\mu_{2X\phi} m_f}{v(s - m_\phi^2)}, \quad C_Z \equiv \frac{g_2 \sqrt{g_1^2 + g_2^2} s_\alpha^2}{2c_{tw}(s - m_Z^2)}, \quad A_{L\nu} = \frac{1}{2}, \quad A_{Ll} = -\frac{1}{2} + s_{tw}^2, \quad A_{Rl} = s_{tw}^2, \\ A_{Lu} &= \frac{1}{2} - \frac{2}{3}s_{tw}^2, \quad A_{Ru} = -\frac{2}{3}s_{tw}^2, \quad A_{Ld} = -\frac{1}{2} + \frac{1}{3}s_{tw}^2, \quad A_{Rd} = \frac{1}{3}s_{tw}^2, \end{aligned} \quad (\text{III.4})$$

where  $C_f = 1$  for  $f = \ell$  and  $C_f = 3$  for  $f = q$ ,  $\mu_{2X\phi} \equiv c_\alpha^2 v \lambda_{\Phi X} + s_\alpha^2 v (\lambda_{\Phi\eta} + \lambda'_{\Phi\eta}) + \sqrt{2} c_\alpha s_\alpha \mu_{\eta X}$ ,  $s \approx M_X^2 (4 + v_{\text{rel}}^2)$  and  $t \approx M_X^2 (-1 + m_f^2/M_X^2 + \sqrt{1 - m_f^2/M_X^2} c_\theta v_{\text{rel}} - v_{\text{rel}}^2/2)$  are the Mandelstam variables.

If we take terms up to the  $v_{\text{rel}}^2$  in  $v_{\text{rel}}$  expansion for all the modes,  $\sigma v_{\text{rel}} \approx a_{\text{eff}} + b_{\text{eff}} v_{\text{rel}}^2$ , we finally obtain the relic density as [46]

$$\Omega h^2 \approx \frac{1.07 \times 10^9 x_f^2}{g_*^{1/2} M_{\text{pl}} [\text{GeV}] (a_{\text{eff}} x_f + 3b_{\text{eff}})}, \quad (\text{III.5})$$

where  $g_* \approx 100$  is the total number of effective relativistic degrees of freedom at the time of freeze-out,  $M_{\text{pl}} = 1.22 \times 10^{19} [\text{GeV}]$  is the Planck mass,  $x_f \approx 25$ , and  $a_{\text{eff}}$ , and  $b_{\text{eff}}$  are coefficients in the  $v_{\text{rel}}^2$  expansion of the annihilation cross section. The observed relic density reported by Planck suggests that  $\Omega h^2 \approx 0.12$  [47].

*Notice here that  $C_Z^2$  (or equivalently  $s_\alpha^4$ ) and  $\mu_{2X\phi}$  should be tiny enough in order to evade the direct detection searches at LUX [48].*

#### IV. NUMERICAL ANALYSIS

For the numerical analysis in this section, we will fix some parameters;  $(M_{N_1}, M_{N_2}, M_{N_3}) = (200, 300, 400)$  GeV and  $(m_{H_1}, m_{H_2}) = (42.7, 550)$  GeV in order to simplify our numerical analysis.<sup>6</sup> Then the range of the other input parameters are randomly

<sup>6</sup> As a consequence, the value of the two-loop function  $F_{II}$  is fixed, otherwise it is too complicated to perform the numerical analysis.

selected by as follows:

$$(y_N)_{ij} \in \pm[0.00001, 0.1], \theta_{1,2,3} \in [0, 2\pi), s_\alpha \in [0.001, 0.1], \beta \in [0.00001, 0.1] \quad (\text{IV.1})$$

$$(\mu_\chi, \mu_{\eta\chi}) \in [10, 1000] \text{ GeV}, m_{H_{1,2}^\pm} \in [70, 1000] \text{ GeV}, \quad (\text{IV.2})$$

where  $y_N$  is symmetric matrix,  $\theta_{1,2,3}$  are arbitrary complex values in the Casas-Ibarra parameters. Notice here  $y_\eta$  should satisfy the perturbative limit;  $y_\eta \lesssim \sqrt{4\pi}$ , and the upper value of  $s_\alpha$  is taken to be 0.1 to suppress the spin independent DM-nucleon scattering cross section so that the direct detection search bounds from LUX or PandaX are satisfied as mentioned before. Among randomly chosen  $10^6$  points, we obtain 1328 allowed points satisfying all the constraints discussed above. In fig. 2, we show a scatter plot of the branching ration of  $\mu \rightarrow e\gamma$  as a function the mixing angle, and we obtain the lower bound on  $-1.5 \lesssim \ln[s_\alpha]$ . This bound comes from the combined result with the neutrino oscillation data and LFVs. If  $s_\alpha$  decreases, the neutrino masses are also smaller. To compensate it, Yukawa coupling (especially  $y_\eta$ ) increases. Since the LFVs do not depend on  $s_\alpha$ , LFVs simply increases when  $y_\eta$  does. Thus  $s_\alpha$  has a lower bound from the upper constraints of LFVs. In fig. 3, we show a scatter plot of muon  $g-2$  as a function the  $H_1^\pm$  mass, where the red points are  $\Delta a_\mu > 0$ , the yellow ones are  $\Delta a_\mu < 0$ . The positive points comes from the contribution of  $a^{\eta\chi}$ . *The maximal scale is typically  $\mathcal{O}(10^{-14})$  that is much less than the measured muon  $g-2$ .* In  $a_R^{\eta\chi}$ , the stringent constraint  $\mu \rightarrow e\gamma$  restricts to be  $(y_\eta)_{11}(y_\chi)_{12} + (y_\eta)_{12}(y_\chi)_{22} + (y_\eta)_{13}(y_\chi)_{32}$ , while muon  $g-2$  is proportional to  $(y_\eta)_{21}(y_\chi)_{12} + (y_\eta)_{22}(y_\chi)_{22} + (y_\eta)_{23}(y_\chi)_{32}$ . In order to obtain sizable muon  $g-2$ , one has to increase  $(y_\eta)_{2i}(i=1-3)$  while decrease  $(y_\eta)_{1i}(i=1-3)$ . However larger  $y_\eta$  increases the negative contribution  $a_\eta$ . Thus  $a_R^{\eta\chi}$  does give a sizable muon  $g-2$ . On the other hand, in  $a_L^{\eta\chi}$ , the same situation has to obtained by exchanging  $y_\eta \leftrightarrow y_\chi$ . Since it also increases the negative contribution  $a_\chi$ . small muon  $g-2$  is obtained from  $a_R^{\eta\chi}$ , too.

## V. FERMI-LAT AT 42.7 GEV

The main mode to the 2 photon process at one-loop level arises from Higgs mediated s channel processes. The contribution from point interaction  $XX^*\eta^+\eta^-$  is very small. The

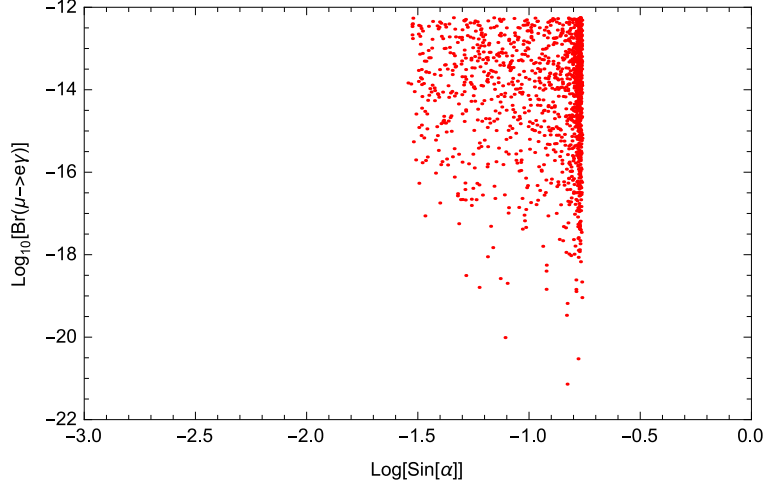


FIG. 2: Scatter plot of the branching ratio of  $\mu \rightarrow e\gamma$  as a function the mixing angle.

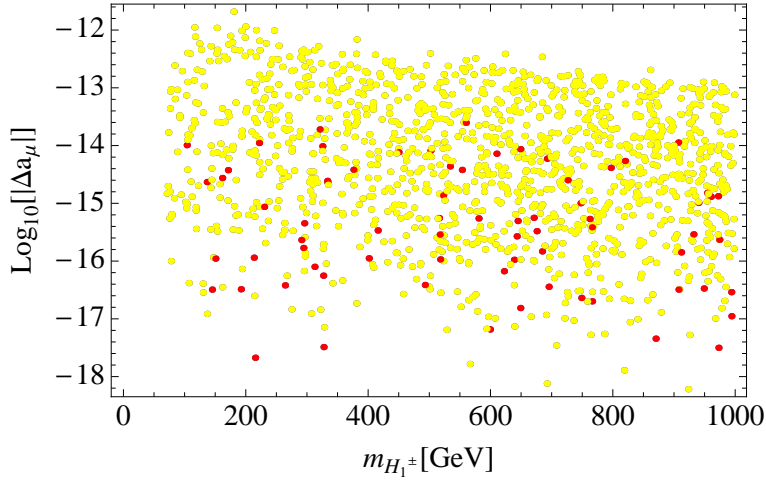


FIG. 3: Scatter plot of the muon  $g-2$  as a function the  $H_1^\pm$  mass, where the red points are  $\Delta a_\mu > 0$ , the yellow ones are  $\Delta a_\mu < 0$ .

cross section is given by [50–55]

$$\begin{aligned}
 (\sigma v)_{\text{FL}} = & \frac{\alpha_{EM}^2 \mu_{2X\phi}^2}{256\pi^3} \frac{1}{(4M_X^2 - m_\phi^2)^2 + m_\phi^2 \Gamma_h^2} \\
 & \times \left( \frac{1}{2} \sum_{i=1}^2 \left( \mu_{2H_i^\pm \phi} v / m_{H_i^\pm}^2 A_0(m_\phi^2 / 4m_{H_i^\pm}^2) \right) + A_{\frac{1}{2}}(m_\phi^2 / 4m_t^2) + A_1(m_\phi^2 / 4m_w^2) \right),
 \end{aligned} \tag{V.1}$$

where  $\mu_{2H_i^\pm\phi}$  is a scalar trilinear coupling between 2  $H_i^\pm$  bosons and Higgs boson,

$$A_0(x) = -\left(1/x - 1/x^2 \arcsin^2 \sqrt{x}\right), \quad (\text{V.2})$$

$$A_{\frac{1}{2}}(x) = \frac{8}{3}\left(1/x + (1/x - 1/x^2) \arcsin^2 \sqrt{x}\right), \quad (\text{V.3})$$

$$A_1(x) = -3\left(1/x + (2/x - 1/x^2) \arcsin^2 \sqrt{x}\right). \quad (\text{V.4})$$

Adapting  $M_X \approx 43$  GeV, the cross section to explain the Fermi-LAT anomaly at 43 GeV should be  $5 \times 10^{-28}$  cm<sup>3</sup>/s or equivalently  $4.27 \times 10^{-11}$  GeV<sup>-2</sup> [36]<sup>7</sup>. If all dimensionful couplings are same value  $\mu$ , we can obtain the following relation,

$$(\sigma v)_{\text{FL}} \approx 9.4 \times 10^{-17} \mu^2 (-4.5 + \mu f(m_{H_1^\pm}, m_{H_2^\pm}))^2 \text{ GeV}^{-4}. \quad (\text{V.5})$$

When  $m_{H_{1,2}^\pm}$  are heavier than 70 GeV,  $f(m_{H_1^\pm}, m_{H_2^\pm})$  is smaller than  $\mathcal{O}(0.01)$  GeV<sup>-1</sup>. Therefore we can find the solution for  $\mu$  within a range of 100 to 1000 GeV. Notice here that  $\chi^\pm$  provides the relaxed constraint of  $\mu$  slightly. Without this field, the typical upper scale of  $\mu$  has to be increased by 1500 GeV.

## VI. SUMMARIES AND DISCUSSIONS

We have explored the possibility to explain the monochromatic Fermi-LAT anomaly at 42.7 GeV dark matter mass in the framework of radiatively induced neutrino mass model at two-loop level. Here we have prepared the Zee-Babu type scenario with  $Z_3$  discrete symmetry, in which we have considered the neutrino oscillation data, lepton flavor violations, and bosonic dark matter candidate. *We have found that the positive muon  $g - 2$ , thanks to  $\chi^\pm$ . And its typical scale is  $\mathcal{O}(10^{-14})$  in our global analysis that is much less than the measured muon  $g - 2$ .* However one could obtain the sizable muon  $g - 2$  by fine-tuning related components among Yukawa couplings  $y_\eta$  and  $y_\chi$  in ref. [56].

A  $\mu - e$  conversion rate has also been estimated and found that the allowed points lies over the wide range, which can be tested in the near future experiment such as PRISM/PRIME.

To explain the Fermi-LAT experiment at 42.7 GeV dark matter mass with  $5 \times 10^{-28}$  cm<sup>3</sup>/s of the non-relativistic cross section, we have used several  $s$ -channel interactions via top fermion,  $W^\pm$  boson, and  $H_{1(2)}^\pm$  boson loops. When  $m_{H_{1,2}^\pm}$  are heavier than 70 GeV,

---

<sup>7</sup> The ref.[49] discusses the Majorana fermionic DM case.

$f(m_{H_1}^\pm, m_{H_2}^\pm)$  is smaller than  $\mathcal{O}(0.01) \text{ GeV}^{-1}$ . Therefore we have found the solution for  $\mu$  within the range of 100 to 1000 GeV. Notice here that  $\chi^\pm$  provides the relaxed constraint of  $\mu$  slightly. Without this field, the typical upper scale of  $\mu$  has to be increased by 1500 GeV.

As another aspect, since DM has nonzero charge under the  $Z_3$  symmetry, it has self-interacting modes that can play an crucial role in relaxing or resolving the dwarf problem around the earth. This topic have already been discussed in several refs. [57].

### Acknowledgments

H. O. is sincerely grateful for all the KIAS members in Korea. This work is supported in part by National Research Foundation of Korea (NRF) Research Grant NRF-2015R1A2A1A05001869 (SB).

### Appendix A: Cholesky decomposition

A symmetric matrix  $M$  is factorized by Cholesky decomposition. The decomposition is as follows;

$$M = \begin{bmatrix} m_{11} & m_{12} & m_{13} \\ m_{12} & m_{22} & m_{23} \\ m_{13} & m_{23} & m_{33} \end{bmatrix} = LL^T, \quad (\text{A.1})$$

where  $L$  is a lower triangular matrix. The explicit form for the matrix  $L$  is

$$L = \begin{bmatrix} l_{11} & 0 & 0 \\ l_{21} & l_{22} & 0 \\ l_{31} & l_{32} & l_{33} \end{bmatrix}, \quad (\text{A.2})$$

$$l_{11} = \pm\sqrt{m_{11}}, \tag{A.3}$$

$$l_{21} = \frac{m_{12}}{l_{11}}, \tag{A.4}$$

$$l_{22} = \pm\sqrt{m_{22} - l_{21}^2}, \tag{A.5}$$

$$l_{31} = \frac{m_{13}}{l_{11}}, \tag{A.6}$$

$$l_{32} = \frac{m_{32} - l_{31}l_{21}}{l_{22}}, \tag{A.7}$$

$$l_{33} = \pm\sqrt{m_{33} - l_{31}^2 - l_{32}^2}. \tag{A.8}$$

We use all positive case.

- 
- [1] A. Zee, Nucl. Phys. B **264**, 99 (1986); K. S. Babu, Phys. Lett. B **203**, 132 (1988).
  - [2] K. S. Babu and C. Macesanu, Phys. Rev. D **67**, 073010 (2003) [hep-ph/0212058].
  - [3] D. Aristizabal Sierra and M. Hirsch, JHEP **0612**, 052 (2006) [hep-ph/0609307].
  - [4] M. Nebot, J. F. Oliver, D. Palao and A. Santamaria, Phys. Rev. D **77**, 093013 (2008) [arXiv:0711.0483 [hep-ph]].
  - [5] D. Schmidt, T. Schwetz and H. Zhang, Nucl. Phys. B **885**, 524 (2014) [arXiv:1402.2251 [hep-ph]].
  - [6] J. Herrero-Garcia, M. Nebot, N. Rius and A. Santamaria, Nucl. Phys. B **885**, 542 (2014) [arXiv:1402.4491 [hep-ph]].
  - [7] H. N. Long and V. V. Vien, Int. J. Mod. Phys. A **29**, no. 13, 1450072 (2014) [arXiv:1405.1622 [hep-ph]].
  - [8] V. Van Vien, H. N. Long and P. N. Thu, arXiv:1407.8286 [hep-ph].
  - [9] M. Aoki, S. Kanemura, T. Shindou and K. Yagyu, JHEP **1007**, 084 (2010) [Erratum-ibid. **1011**, 049 (2010)] [arXiv:1005.5159 [hep-ph]].
  - [10] M. Lindner, D. Schmidt and T. Schwetz, Phys. Lett. B **705**, 324 (2011) [arXiv:1105.4626 [hep-ph]].
  - [11] S. Baek, P. Ko, H. Okada and E. Senaha, JHEP **1409**, 153 (2014) [arXiv:1209.1685 [hep-ph]].
  - [12] M. Aoki, J. Kubo and H. Takano, Phys. Rev. D **87**, no. 11, 116001 (2013) [arXiv:1302.3936 [hep-ph]].
  - [13] Y. Kajiyama, H. Okada and K. Yagyu, Nucl. Phys. B **874**, 198 (2013) [arXiv:1303.3463 [hep-ph]].

- ph]].
- [14] Y. Kajiyama, H. Okada and T. Toma, Phys. Rev. D **88**, 015029 (2013) [arXiv:1303.7356].
  - [15] S. Baek, H. Okada and T. Toma, JCAP **1406**, 027 (2014) [arXiv:1312.3761 [hep-ph]].
  - [16] H. Okada, arXiv:1404.0280 [hep-ph].
  - [17] H. Okada, T. Toma and K. Yagyu, Phys. Rev. D **90**, no. 9, 095005 (2014) [arXiv:1408.0961 [hep-ph]].
  - [18] H. Okada, arXiv:1503.04557 [hep-ph].
  - [19] C. Q. Geng and L. H. Tsai, arXiv:1503.06987 [hep-ph].
  - [20] S. Kashiwase, H. Okada, Y. Orikasa and T. Toma, Int. J. Mod. Phys. A **31**, no. 20n21, 1650121 (2016) doi:10.1142/S0217751X16501219 [arXiv:1505.04665 [hep-ph]].
  - [21] M. Aoki and T. Toma, JCAP **1409**, 016 (2014) [arXiv:1405.5870 [hep-ph]].
  - [22] S. Baek, H. Okada and T. Toma, Phys. Lett. B **732**, 85 (2014) [arXiv:1401.6921 [hep-ph]].
  - [23] H. Okada and Y. Orikasa, Phys. Rev. D **93**, no. 1, 013008 (2016) doi:10.1103/PhysRevD.93.013008 [arXiv:1509.04068 [hep-ph]].
  - [24] D. Aristizabal Sierra, A. Degee, L. Dorame and M. Hirsch, JHEP **1503**, 040 (2015) [arXiv:1411.7038 [hep-ph]].
  - [25] T. Nomura and H. Okada, Phys. Lett. B **756**, 295 (2016) [arXiv:1601.07339 [hep-ph]].
  - [26] T. Nomura, H. Okada and Y. Orikasa, arXiv:1602.08302 [hep-ph].
  - [27] C. Bonilla, E. Ma, E. Peinado and J. W. F. Valle, arXiv:1607.03931 [hep-ph].
  - [28] M. Kohda, H. Sugiyama and K. Tsumura, Phys. Lett. B **718**, 1436 (2013) [arXiv:1210.5622 [hep-ph]].
  - [29] B. Dasgupta, E. Ma and K. Tsumura, Phys. Rev. D **89**, 041702 (2014) [arXiv:1308.4138 [hep-ph]].
  - [30] S. Baek, JHEP **1508**, 023 (2015) doi:10.1007/JHEP08(2015)023 [arXiv:1410.1992 [hep-ph]].
  - [31] T. Nomura and H. Okada, Phys. Rev. D **94**, 075021 (2016) doi:10.1103/PhysRevD.94.075021 [arXiv:1607.04952 [hep-ph]].
  - [32] T. Nomura and H. Okada, arXiv:1609.01504 [hep-ph].
  - [33] T. Nomura, H. Okada and Y. Orikasa, Phys. Rev. D **94**, no. 11, 115018 (2016) doi:10.1103/PhysRevD.94.115018 [arXiv:1610.04729 [hep-ph]].
  - [34] Z. Liu and P. H. Gu, arXiv:1611.02094 [hep-ph].
  - [35] K. A. Olive *et al.* [Particle Data Group], Chin. Phys. C **38**, 090001 (2014).

- [36] Y. F. Liang *et al.*, Phys. Rev. D **93**, no. 10, 103525 (2016) doi:10.1103/PhysRevD.93.103525 [arXiv:1602.06527 [astro-ph.HE]].
- [37] R. J. Barlow, Nucl. Phys. Proc. Suppl. **218**, 44 (2011). doi:10.1016/j.nuclphysbps.2011.06.009
- [38] Z. Maki, M. Nakagawa and S. Sakata, Prog. Theor. Phys. **28**, 870 (1962). doi:10.1143/PTP.28.870
- [39] M. Lindner, M. Platscher and F. S. Queiroz, arXiv:1610.06587 [hep-ph].
- [40] C. Guo, S. Y. Guo, Z. L. Han, B. Li and Y. Liao, arXiv:1701.02463 [hep-ph].
- [41] D. V. Forero, M. Tortola and J. W. F. Valle, Phys. Rev. D **90**, no. 9, 093006 (2014) doi:10.1103/PhysRevD.90.093006 [arXiv:1405.7540 [hep-ph]].
- [42] E. V. Hungerford [COMET Collaboration], AIP Conf. Proc. **1182**, 694 (2009).
- [43] C. Dohmen *et al.* [SINDRUM II Collaboration], Phys. Lett. B **317**, 631 (1993).
- [44] W. H. Bertl *et al.* [SINDRUM II Collaboration], Eur. Phys. J. C **47**, 337 (2006).
- [45] W. Honecker *et al.* [SINDRUM II Collaboration], Phys. Rev. Lett. **76**, 200 (1996).
- [46] K. Griest and D. Seckel, Phys. Rev. D **43**, 3191 (1991). doi:10.1103/PhysRevD.43.3191
- [47] P. A. R. Ade *et al.* [Planck Collaboration], Astron. Astrophys. **571**, A16 (2014) doi:10.1051/0004-6361/201321591 [arXiv:1303.5076 [astro-ph.CO]].
- [48] D. S. Akerib *et al.*, arXiv:1608.07648 [astro-ph.CO].
- [49] L. Feng, Y. F. Liang, T. K. Dong and Y. Z. Fan, Phys. Rev. D **94**, no. 4, 043535 (2016) doi:10.1103/PhysRevD.94.043535 [arXiv:1608.04056 [hep-ph]].
- [50] J. R. Ellis, M. K. Gaillard and D. V. Nanopoulos, Nucl. Phys. B **106**, 292 (1976). doi:10.1016/0550-3213(76)90382-5
- [51] M. A. Shifman, A. I. Vainshtein, M. B. Voloshin and V. I. Zakharov, Sov. J. Nucl. Phys. **30**, 711 (1979) [Yad. Fiz. **30**, 1368 (1979)].
- [52] A. Djouadi, Phys. Rept. **457**, 1 (2008) doi:10.1016/j.physrep.2007.10.004 [hep-ph/0503172].
- [53] R. Gastmans, S. L. Wu and T. T. Wu, arXiv:1108.5872 [hep-ph].
- [54] M. Carena, I. Low and C. E. M. Wagner, JHEP **1208**, 060 (2012) doi:10.1007/JHEP08(2012)060 [arXiv:1206.1082 [hep-ph]].
- [55] K. Nishiwaki, H. Okada and Y. Orikasa, Phys. Rev. D **92**, no. 9, 093013 (2015) doi:10.1103/PhysRevD.92.093013 [arXiv:1507.02412 [hep-ph]].
- [56] T. Hambye, K. Kannike, E. Ma and M. Raidal, Phys. Rev. D **75**, 095003 (2007) doi:10.1103/PhysRevD.75.095003 [hep-ph/0609228].

- [57] S. Tulin, H. B. Yu and K. M. Zurek, *Phys. Rev. D* **87**, no. 11, 115007 (2013)  
doi:10.1103/PhysRevD.87.115007 [arXiv:1302.3898 [hep-ph]].